

## Supplementary Materials:

# Bis(triphenylphosphine)iminium Salts of Dioxothiadiazole Radical Anions: Preparation, Crystal Structures, and Magnetic Properties

Paweł Pakulski, Mirosław Arczyński \* and Dawid Pinkowicz \*

Jagiellonian University, Faculty of Chemistry, Gronostajowa 2, 30-387 Kraków, Poland;  
pawel.pakulski@doctoral.uj.edu.pl

\* Correspondence: miroslaw.arczynski@doctoral.uj.edu.pl (M.A.); dawid.pinkowicz@uj.edu.pl (D.P.)

**Table S1.** Details of single crystal X-Ray data and structural refinement for **PPN(L)**, **S2** **PPN(BrL)** and **PPN(4,7-L)** **PPN(diBrL)**, **diBrL** and **BrL**.

Figure S1. Illustration of molecular stacks in **BrL** with marked short  $\sigma$ - $\pi$  contacts a) and fragment of a supramolecular layer with marked contacts that are shorter than the sum of the Van der Waals radii b) (made using Mercury program). **S3**

Figure S2. Illustration of crystal packing of **diBrL**. The supramolecular chains of parallel hydrogen bonded dimers run through the structure interacting via  $\pi$ -orbitals and short contacts with bromine atoms. **S4**

Figure S3. Illustration of **PPN(BrL)** supramolecular layers. Contacts between BrL anions that are shorter than the sum of the Van der Waals radii. **S5**

Figure S4. NMR spectrum of 3-bromo-1,10-phenanthroline-5,6-dione. **S6**

Figure S5. NMR spectrum of 5-bromo-[1,2,5]thiadiazolo[3,4-f][1,10]phenanthroline 2,2-dioxide **BrL**. **S7**

Figure S6. NMR spectrum of 3,8-dibromo-1,10-phenanthroline-5,6-dione. **S8**

Figure S7. NMR spectrum of 5,10-dibromo-[1,2,5]thiadiazolo[3,4-f][1,10]phenanthroline 2,2-dioxide **diBrL**. **S9**

Figure S8. Superexchange coupling scheme in **PPN(4,7-L)** (a), **PPN(BrL)** (b), **PPN(L)** (c) and **PPN(diBrL)** (d). The green ovals and dotted lines indicate the magnetic interaction pathways taken into account in the fitting of the magnetic data. In the case of **PPN(diBrL)** (d) two interaction pathways are considered:  $J_{12}$  and  $J_{34}$  with the assumption that  $J_{12} \gg J_{34}$ . **S10**

Figure S9. Illustration of supramolecular stack of diBrL anions in the crystal structure of **PPN(diBrL)**. The molecules are color coded to depict different intermolecular **S11**

contacts between them. The asymmetric unit contains one green and one blue molecule.

The most efficient  $\pi$ - $\pi$  orbitals overlap is between light blue and navy blue molecules.

**Table S1.** Details of single crystal X-Ray data and structural refinement for PPN(L), PPN(BrL), PPN(4,7-L) PPN(diBrL), diBrL and BrL.

		PPN(4,7-L)	PPN(BrL)	PPN(L)	BrL	diBrL	PPN(diBrL)*
CCDC deposition number		1882328	1882331	1882329	1882326	1882327	1882330
formula		C <sub>48</sub> H <sub>36</sub> N <sub>5</sub> P <sub>2</sub> O <sub>2</sub> S	C <sub>54</sub> H <sub>30</sub> N <sub>5</sub> P <sub>2</sub> BrO <sub>3.5</sub>	C <sub>54</sub> H <sub>49</sub> N <sub>5</sub> P <sub>2</sub> O <sub>5.25</sub> S	C <sub>12</sub> H <sub>5</sub> BrN <sub>4</sub> O <sub>2</sub> S	C <sub>12</sub> H <sub>4</sub> Br <sub>2</sub> N <sub>4</sub> O <sub>2</sub> S	C <sub>48</sub> H <sub>34</sub> Br <sub>2</sub> N <sub>5</sub> O <sub>2</sub> P <sub>2</sub> S
FW [g·mol <sup>-1</sup> ]		808.82	978.74	929.98	349.17	428.07	966.62
T [K]		120(1)	120(1)	120(1)	120(1)	120(1)	117(2)
wavelength (radiation)		0.71073 Å (Mo K $\alpha$ )	0.71073 Å (Mo K $\alpha$ )	0.71073 Å (Mo K $\alpha$ )	0.71073 Å (Mo K $\alpha$ )	0.71073 Å (Mo K $\alpha$ )	0.71073 Å (Mo K $\alpha$ )
space group		P2 <sub>1</sub> /c	P-1	P-1	P-1	P2 <sub>1</sub> /c	P-1
unit cell	a [Å]	9.4226 (3)	11.525 (3)	11.451 (8)	5.0133 (8)	6.7679 (9)	14.3233(6)
	b [Å]	16.9415 (4)	14.122 (4)	14.378 (8)	11.1415 (19)	8.6646 (13)	15.7838(7)
	c [Å]	26.2571 (7)	16.056 (4)	15.701 (12)	11.3099 (18)	22.801 (3)	21.0047(9)
	$\alpha$ (°)	90.0	70.664 (8)	112.01 (3)	69.183 (4)	90.0	92.144(2)
	$\beta$ (°)	98.046 (2)	75.272 (9)	102.19 (4)	87.853 (4)	96.888 (4)	91.480(2)
	$\gamma$ (°)	90.0	89.129 (10)	90.15 (3)	85.141 (4)	90.0	116.651(2)
$V$ [Å <sup>3</sup> ]		3997.9 (1)	2377.8 (11)	2333 (3)	588.34 (17)	1327.4 (3)	4236.3(3)
Z		4	2	2	2	4	4
density [g·cm <sup>-3</sup> ]		1.376	1.367	1.324	1.971	2.142	1.516
abs. coeff. $\mu$ [mm <sup>-1</sup> ]		0.214	1.03	0.19	3.68	6.27	2.086
crystal description		Deep-Purple Block	Deep-Purple Plate	Deep-Purple plate	Yellow Needle	Orange Needle	Deep-Purple Plate
crystal size [mm <sup>3</sup> ]		0.14 × 0.14 × 0.1	0.39 × 0.26 × 0.04	0.37 × 0.33 × 0.1	0.18 × 0.06 × 0.03	0.14 × 0.04 × 0.01	0.09 × 0.08 × 0.02
$F(000)$		1684	996	976	344	824	1956
collection $\theta$ range [deg]		3.362 – 25.048	3.1 – 27.9	2.7 – 27.5	3.2 – 24.9	2.5 – 26.5	2.4 – 26.45
collected reflections		29322	24850	18355	2847	8552	24318
independent reflections		6728	11119	10293	1996	2713	18276
$R_{\text{int}}$		0.0447	0.075	0.021	0.035	0.085	twin
completeness [%]		97.3	98.1	97.4	98.1	98.7	99.8
refinement method		Full-matrix least-squares on $F^2$					
data/restraints/parameters		6728/0/523	11119/5/563	10293/21/608	1996/0/181	2713/48/190	24318/0/1082
GOF on $F^2$		1.015	1.029	1.058	1.012	1.022	1.07
$R_1$ [ $I > 2\sigma(I)$ ]**		$R_1 = 0.0401$	$R_1 = 0.068$	$R_1 = 0.061$	$R_1 = 0.044$	$R_1 = 0.048$	$R_1 = 0.0555$
$wR_2$ [all data]		$wR_2 = 0.0936$	$wR_2 = 0.195$	$wR_2 = 0.163$	$wR_2 = 0.109$	$wR_2 = 0.089$	$wR_2 = 0.1337$
Max./min. residual density [e·Å <sup>-3</sup> ]		0.292	1.06	0.68	0.78	0.82	0.783
		-0.423	-1.03	-0.63	-0.61	-0.87	-0.966

\* Refined as a two component twin with scales: 0.6227(6) and 0.3773(6)

\*\*  $R_1 = \sum[|F_0| - |F_c|]/\sum|F_0|$ ;  $wR_2 = \{\sum[w(F_o^2 - F_c^2)^2]/\sum[w(F_o^2)^2]\}^{1/2}$ ;  $w = 1/[o^2F^2 + (0.0323P)^2 + 18.2463P]$ ;  $P = (F^2 + 2F_c^2)/3$

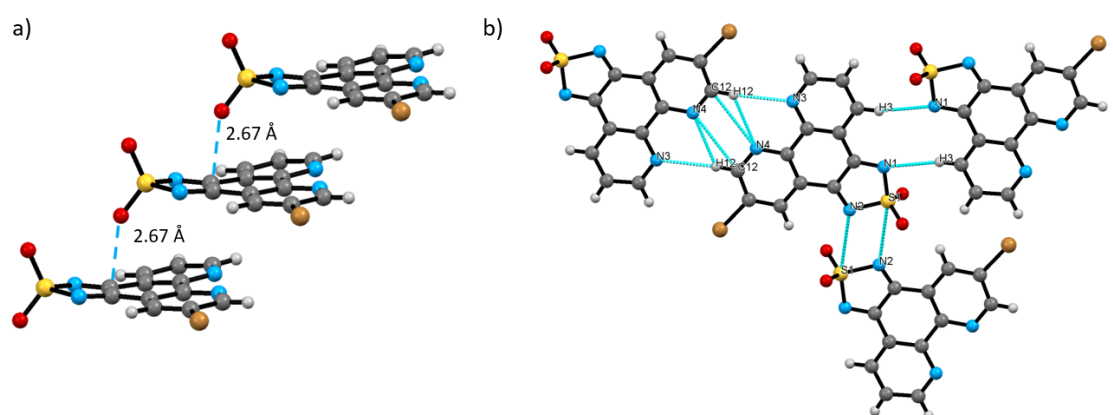


Figure S1. Illustration of molecular stacks in **BrL** with marked short  $\sigma$ - $\pi$  contacts a) and fragment of a supramolecular layer with marked contacts that are shorter than the sum of the Van der Waals radii b) (made using Mercury program).

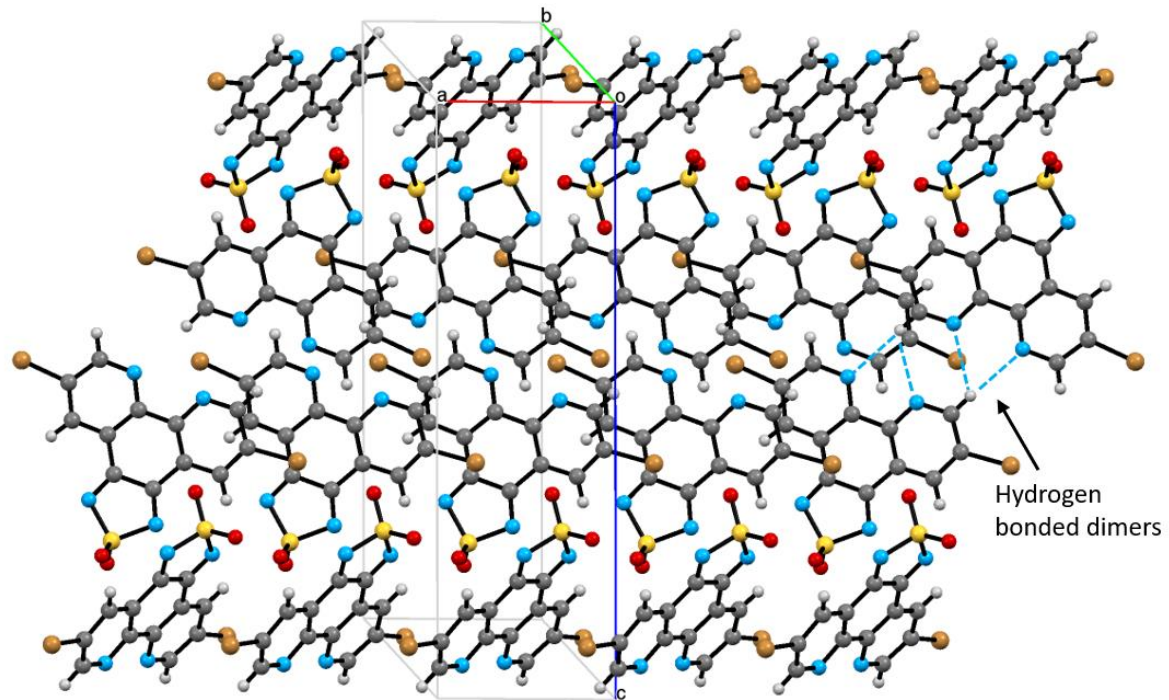


Figure S2. Illustration of crystal packing of **diBrL**. The supramolecular chains of parallel hydrogen bonded dimers run through the structure interacting via  $\pi$ -orbitals and short contacts with Bromine atoms.

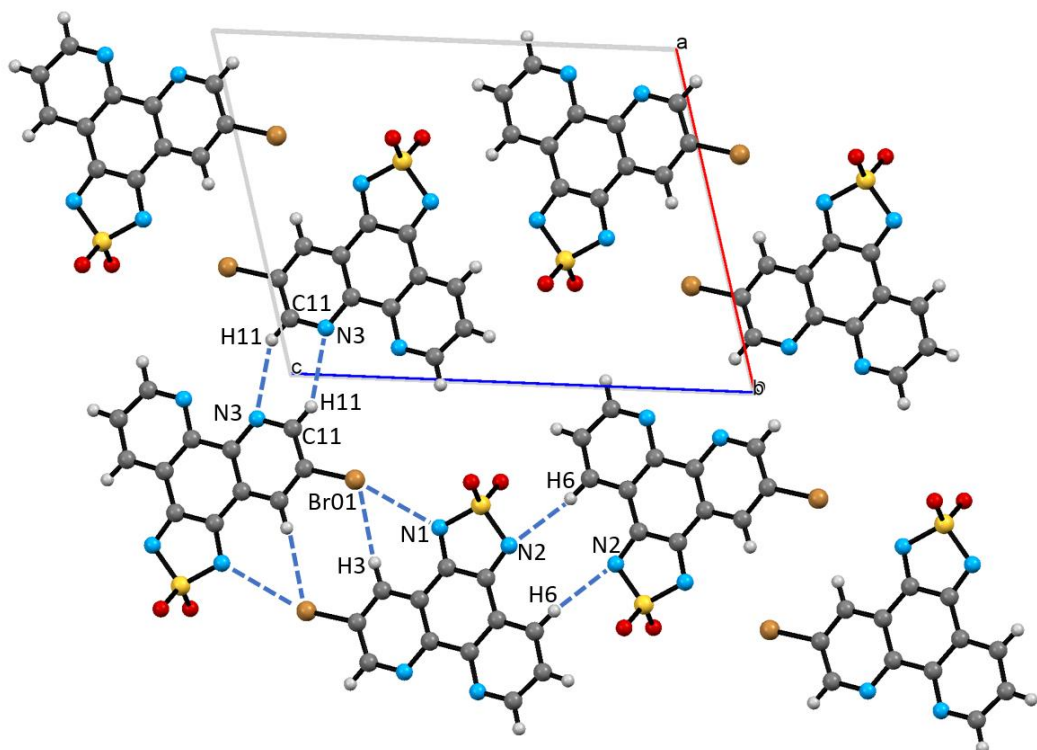


Figure S3. Illustration of **PPN(BrL)** supramolecular layers. Contacts between BrL anions that are shorter than the sum of the Van der Waals radii.

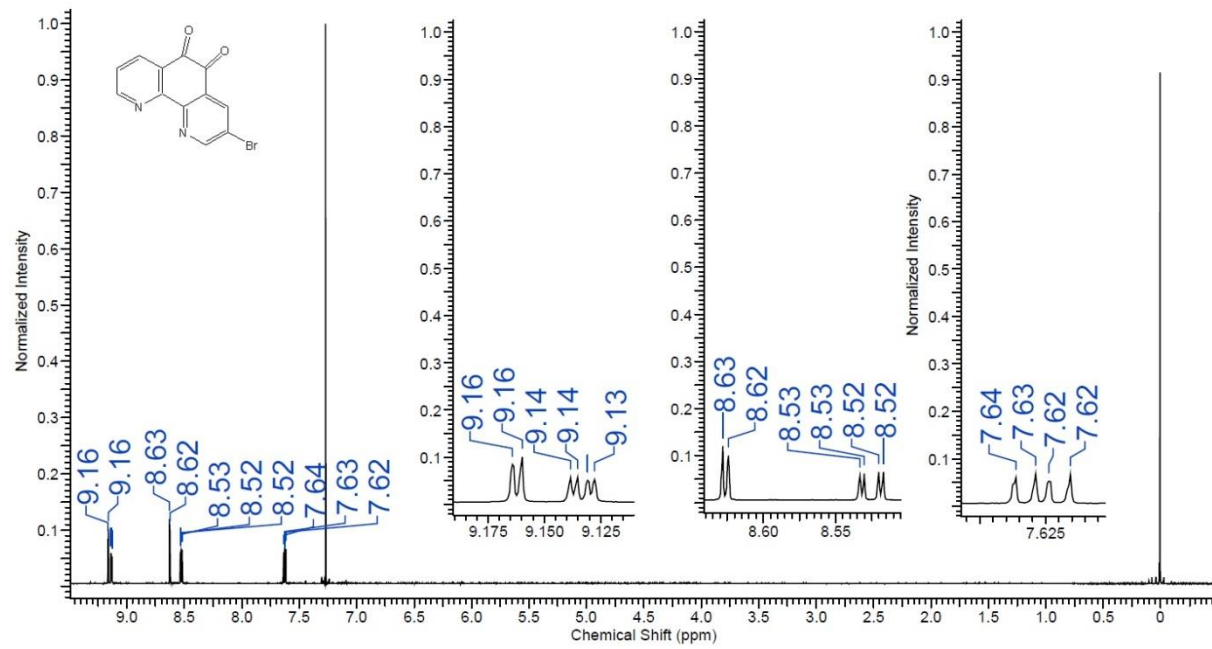


Figure S4. NMR spectrum of 3-bromo-1,10-phenanthroline-5,6-dione.

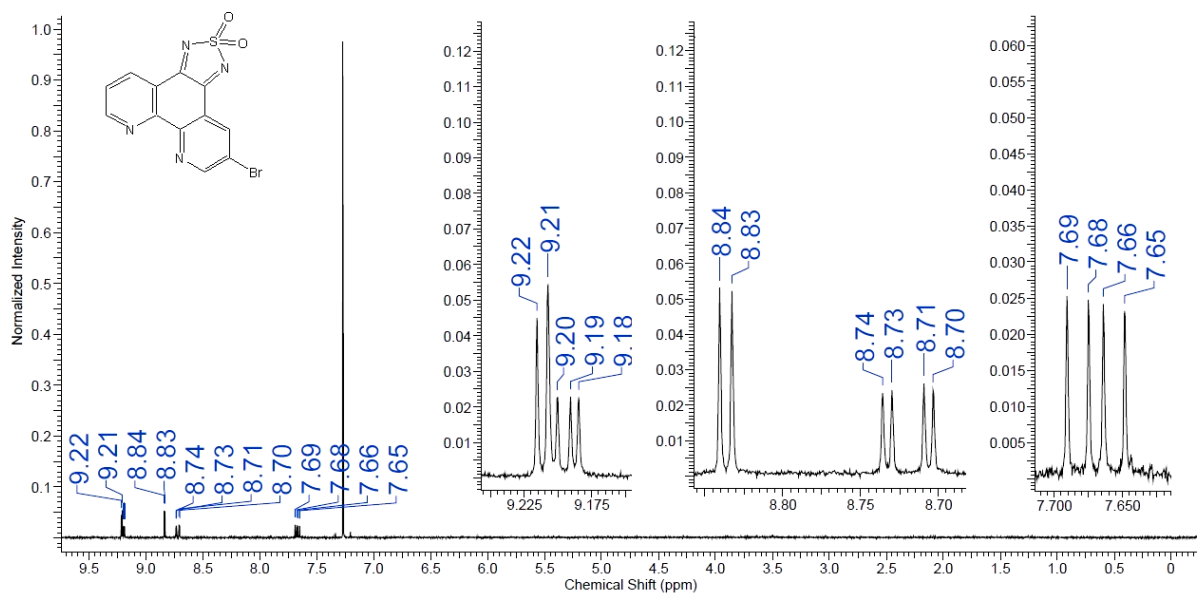


Figure S5. NMR spectrum of 5-bromo-[1,2,5]thiadiazolo[3,4-f][1,10]phenanthroline 2,2-dioxide **BrL**.

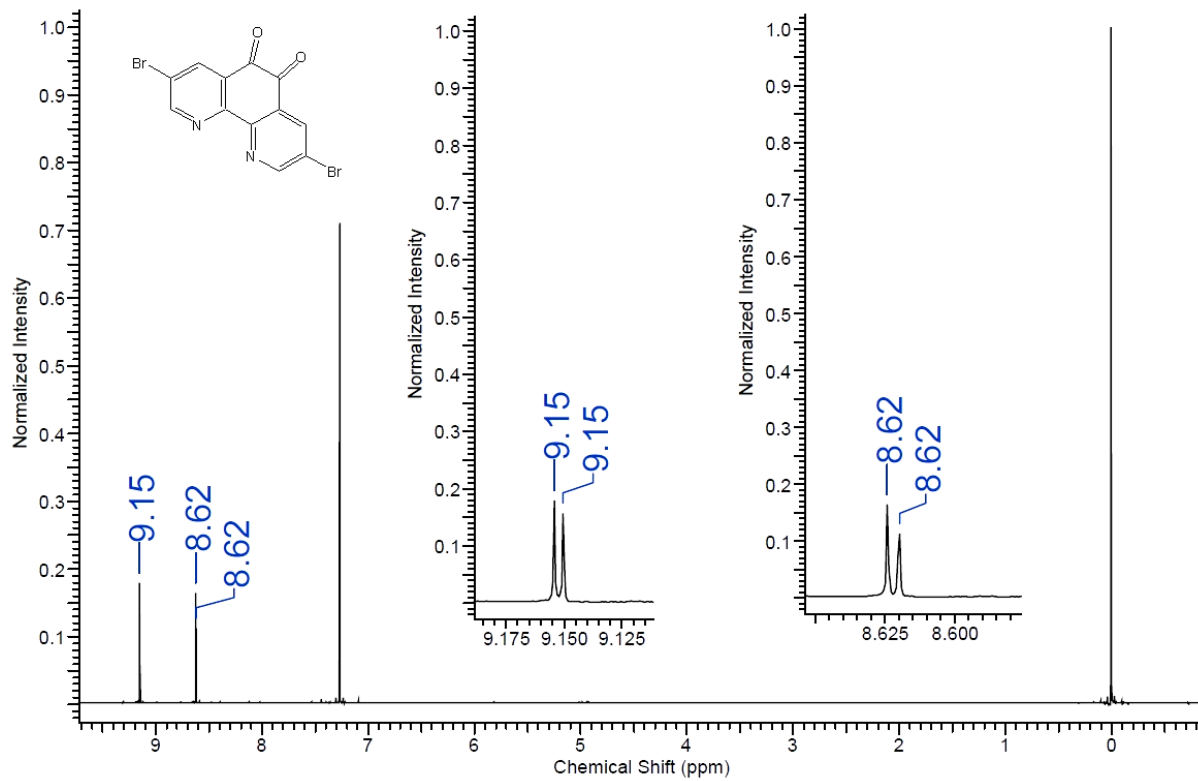


Figure S6. NMR spectrum of 3,8-dibromo-1,10-phenanthroline-5,6-dione.

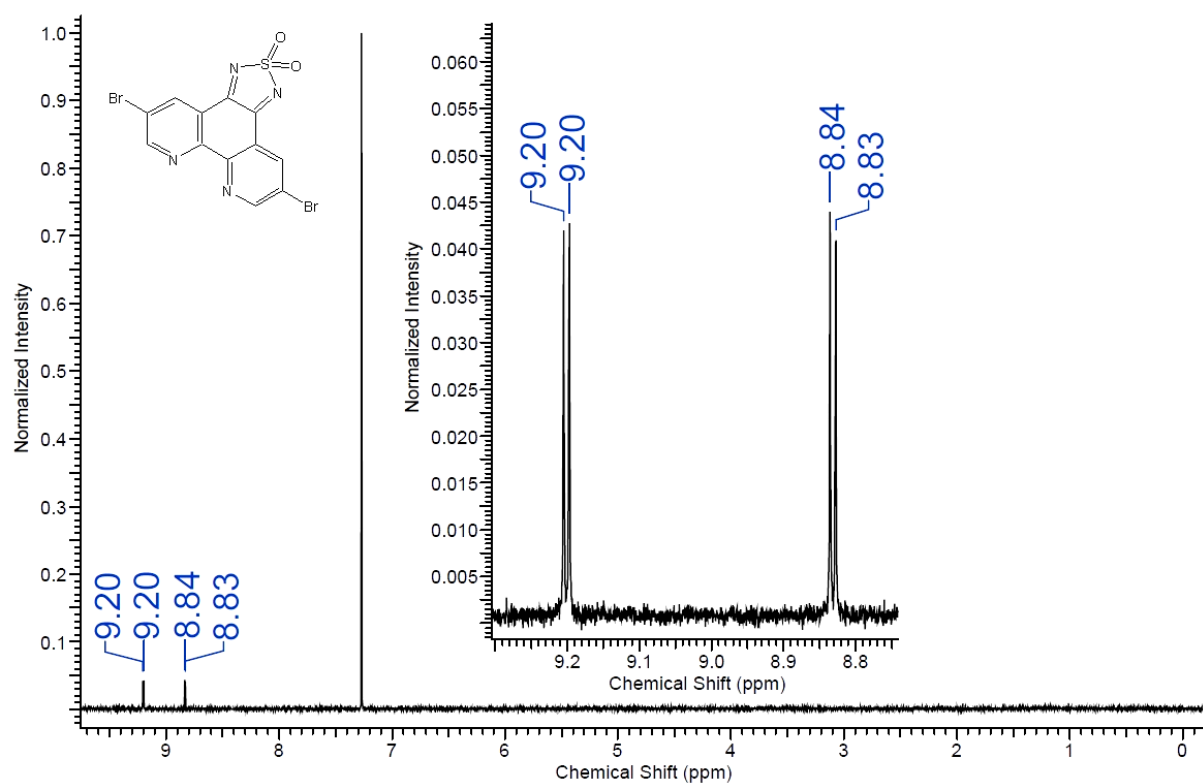


Figure S7. NMR spectrum of 5,10-dibromo-[1,2,5]thiadiazolo[3,4-f][1,10]phenanthroline 2,2-dioxide **diBrL**.

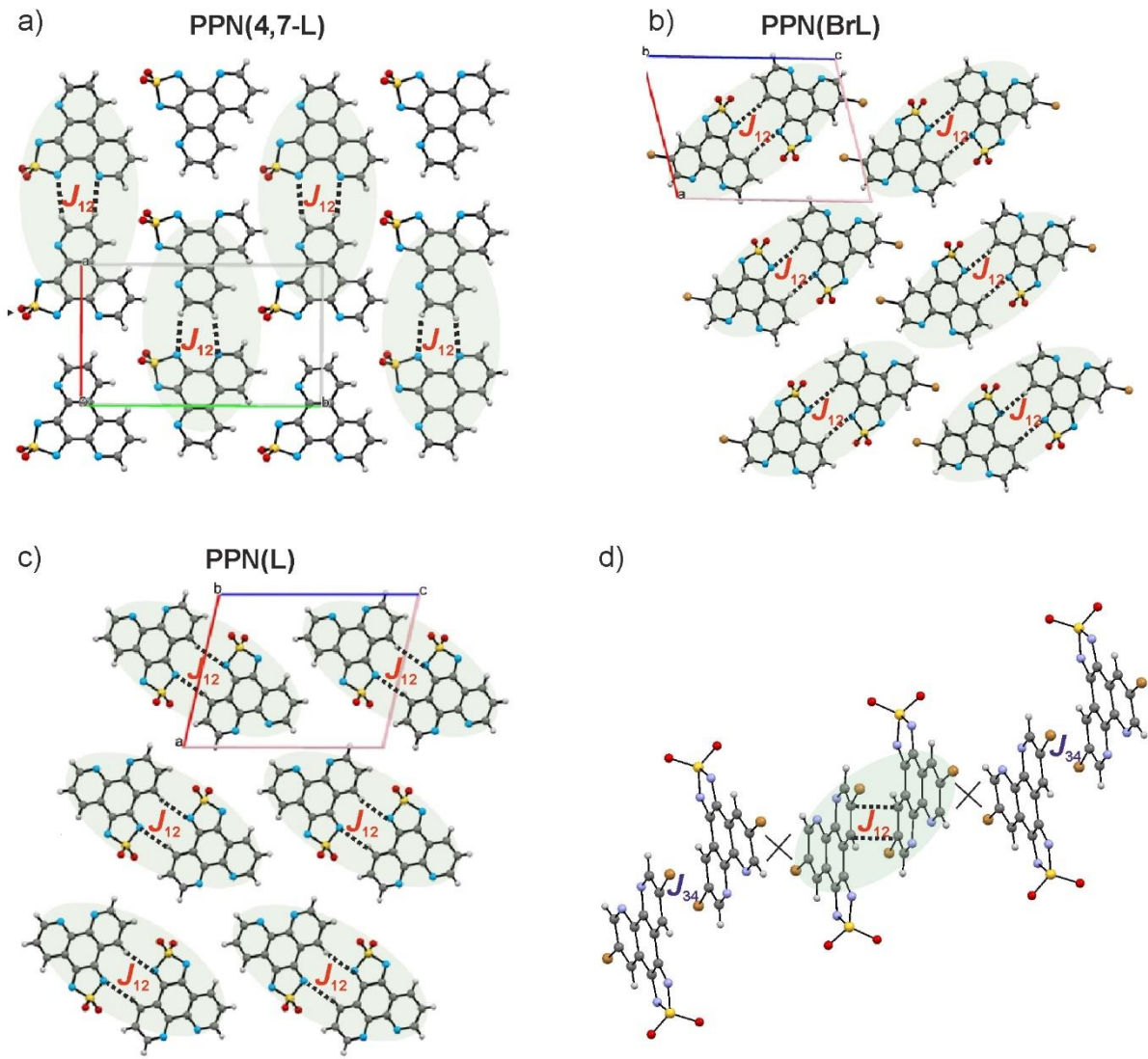


Figure S8. Superexchange coupling scheme in **PPN(4,7-L)** (a), **PPN(BrL)** (b), **PPN(L)** (c) and **PPN(diBrL)** (d). The green ovals and dotted lines indicate the magnetic interaction pathways taken into account in the fitting of the magnetic data. In the case of **PPN(diBrL)** (d) two interaction pathways are considered:  $J_{12}$  and  $J_{34}$  with the assumption that  $J_{12} \gg J_{34}$ .

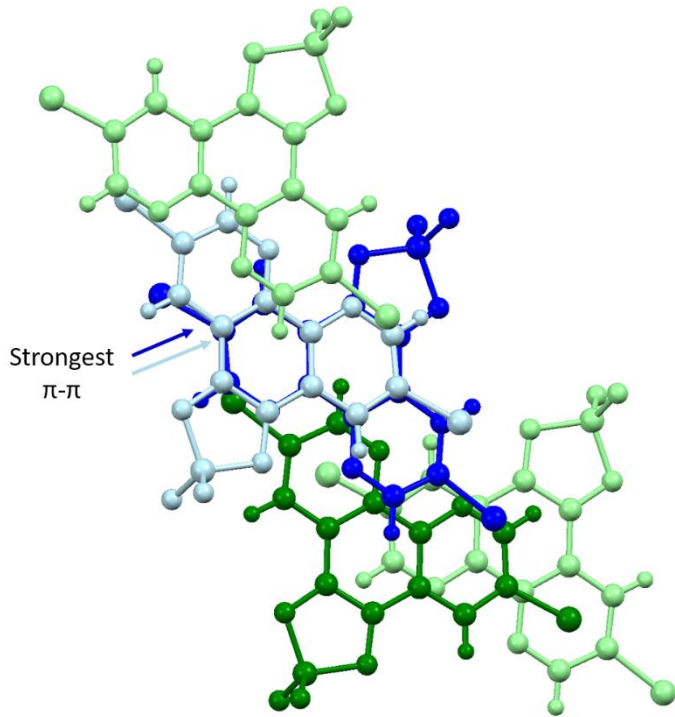


Figure S9. Illustration of supramolecular stack of diBrL anions in the crystal structure of PPN(diBrL). The molecules are color coded to depict different intermolecular contacts between them. The asymmetric unit contains one green and one blue molecule. The most efficient  $\pi$ - $\pi$  orbitals overlap is between light blue and navy blue molecules.